PAPER

Mobile monitoring along a street canyon and stationary forest air monitoring of formaldehyde by means of a micro gas analysis system

Kei Toda,[*a] **Wataru Tokunaga,**[a] **Yosuke Gushiken,**[a] **Kazutoshi Hirota,**[a] **Teppei Nose,**[a] **Daisaku Suda,**[a] **Jun Nagai**[a] **and Shin-Ichi Ohira**[a]

A micro gas analysis system (μGAS) was developed for mobile monitoring and continuous measurements of atmospheric HCHO. HCHO gas was trapped into an absorbing/reaction solution continuously using a microchannel scrubber in which the microchannels were patterned in a honeycomb structure to form a

10 wide absorbing area with a thin absorbing solution layer. Fluorescence was monitored after reaction of the collected HCHO with 2,4-pentanedione (PD) in the presence of acetic acid/ammonium acetate. The system was portable, battery-driven, highly sensitive (limit of detection = 0.01 ppbv) and had good time resolution (response time 50 s). The results revealed that the PD chemistry was subject to interference from O_3. The mechanism of this interference was investigated and the problem was addressed by

15 incorporating a wet denuder. Mobile monitoring was performed along traffic roads, and elevated HCHO levels in a street canyon were evident upon mapping of the obtained data. The system was also applied to stationary monitoring in a forest in which HCHO formed naturally via reaction of biogenic compounds with oxidants. Concentrations of a few ppbv-HCHO and several-tens of ppbv of O_3 were then simultaneously monitored with the μGAS in forest air monitoring campaigns. The obtained 1-h average

20 data were compared with those obtained by 1-h impinger collection and off site GC-MS analysis after derivatization with *o*-(2,3,4,5,6-pentafluorobenzyl) hydroxylamine (PFBOA). From the obtained data in forest, daily variations of chemical HCHO production and loss are discussed.

Introduction

Formaldehyde (HCHO) is an important volatile compound in the
25 atmosphere, as well as in indoor air.[1] In urban areas, HCHO is primarily emitted from vehicles. For example, Zhao et al.[2] reported that a gasoline engine vehicle emits HCHO at a rate of 0.6 mg km^{-1}. On the other hand, HCHO is formed in rural and natural ecosystems via photochemical reaction of biogenic
30 volatile organic compounds (BVOCs).[3,4] Gaseous HCHO is decomposed by photolysis and OH radicals.[5] HCHO is also a precursor to HO_2 radical and ozone in gas phase reactions,[6] as well as to formic acid in aqueous reactions such as aerosols and rain drops.[7-9] Thus, HCHO is formed via several pathways and
35 has multiple fates. Indeed, HCHO is a hub-compound of atmospheric reactions, which makes HCHO analysis extremely attractive to promote further understanding atmospheric chemistry and its risks to human health.

Currently, the most popular method for analysis of gaseous
40 HCHO is collection using a silica gel cartridge impregnated with 2,4-dinitrophenylhydrazine (DNPH) followed by organic solvent extraction and high performance liquid chromatography (HPLC).[4,10,11] Although the DNPH-HPLC method is convenient for obtaining spot data for indoor analysis, it requires a long

45 collection time and is not suitable for atmospheric trace level analysis. Gu et al. recently proposed a novel method in which a HCHO was trapped directly by a new sorbent known as a metal–organic framework, after which thermal desorption was used to introduce the trapped HCHO to the gas chromatograph.[12] A good
50 limit of detection (0.5 ppbv) was obtained by 10 min of sampling and laboratory instrumental analysis using this technique. Many continuous methods for detailed analysis have been reported. These methods utilize continuous collection devices such as coil denuders,[13-16] and membrane based annular diffusion scrubbers
55 with Nafion tubes,[17] porous polypropylene tubes,[18] or porous polytetrafluoroethylene (PTFE) tubes.[19] HCHO is extremely sticky and easily collected into aqueous absorbing solution due to its high Henry's law constant of 5020 M atm^{-1} at 25°C.[20] Chemical determinations of HCHO collected in the aqueous
60 phase are conducted using DNPH,[19] 3-methyl-2-benzothiazolone (MBTH)[21] for spectrophotometric analysis and 2,4-pentanedione (PD) (acetyl acetone),[22,23] 1,3-cyclohexanedione (CHD),[24] and 5,5-dimethylcyclohexane-1,3-dione (dimedone)[25] for fluorometric analysis. Dasgupta et al. examined several reactions
65 for HCHO analysis and favored PD chemistry.[26] In this study, we propose a novel micro gas analysis system (μGAS) to determine trace levels of HCHO in the field using PD chemistry. The portable μGAS was developed for field measurement of H_2S and SO_2[27] and on site medical diagnostics[28] and treatments.[29] Special
70 techniques for μGAS analysis have been developed including pneumatic/electroosmotic flow control[30] and on-site calibration with a micro standard gas generator.[31] Miniaturized gas analyzers

a Department of Chemistry, Kumamoto University, Kurokami 2-39-1, Kumamoto 860-8555, Japan. Tel: +81-96-342-3389; Email: todakei@sci.kumamoto-u.ac.jp

are currently of considerable interest, and their applications range from atmospheric monitoring to medical diagnosis and counterterrorism.[32,33]

In this study, HCHO analysis using the μGAS was investigated and applied to mobile analysis in a street canyon. Stationary simultaneous analyses were repeated in two years in a forest for isoprene, monoterpenes, organic acids, NO_x and O_3,[34] together with HCHO. During the forest study, slight interference from O_3 was observed, and this interference was not negligible during trace HCHO analysis when the O_3 concentration was high, as in situations when oxidant or photochemical smog warnings were occurring. In this work, the mechanisms of O_3 interference and countermeasures for this problem were investigated. The compensated HCHO results in a few ppbv levels agreed well with data obtained by conventional 1 h collection followed by derivatization with o-(2,3,4,5,6-pentafluorobenzyl) hydroxyl-amine (PFBOA) and gas chromatography mass spectrometry (GC-MS). Based on the results obtained for the forest, the contributions of each reaction of BVOC with an oxidant to form HCHO are discussed. Daily variations in the HCHO formation and loss are also estimated.

Experimental

Reagents

Working absorbing/reaction solution was prepared from two stock solutions, 0.03 M PD (Tokyo Kasei, Tokyo, Japan), and 0.75 M acetic acid + 6 M ammonium acetate (both from Nacalai Tesuque, Kyoto, Japan). The working solution was prepared immediately before use by mixing the two stock solutions and milli-Q water (1: 1: 1) to give final concentrations of PD, acetic acid and ammonium acetate of 0.01, 0.25 and 2 M, respectively.

HCHO test gas was prepared as previously described.[21] Briefly, HCHO aqueous solution (0.1~1 mM, 40 mL) in an impinger was placed in a 20°C water bath and then bubbled with purified air applied at a rate of 200 mL min⁻¹. The bubbler temperature was set lower than the ambient temperature to prevent water condensation in the air line. Dong and Dasgupta demonstrated a concrete relationship between vapor pressure P_{HCHO} (atm) and aqueous concentration [HCHO] (M) as a function of the absolute temperature T as eq. 1 in the range from 0.01 mM (3.3 ppbv) to 6.9 mM (1.3 ppmv).[35]

$$[HCHO] = 10^{(4538/T-11.34)} \times P_{HCHO}^{(252.2/T+0.2088)} \quad (1)$$

Note that the exponential relationship fits to their experimental, not linear relationship, due to formation of hydrated *gem*-diol.[36] According to eq. 1, 0.10 ppmv HCHO vapor was obtained by bubbling 0.53 mM HCHO solution at 20°C and 1.0 atm. The outlet gas was diluted just after the impinger with purified dry air to obtain the desired concentration. It should be noted that the aqueous HCHO concentration decreases very gradually due to vaporization; specifically, the HCHO generation rate decreases 0.25% h⁻¹ under these conditions. Therefore, the HCHO vapor generator solution was exchanged every 8 h or prepared immediately before use.

System setup and procedure

Diagrams of the systems for mobile and stationary monitoring are shown in Fig. 1a and b, respectively. HCHO gas was collected into the absorbing/reaction solution using a microchannel scrubber[28] in which the microchannels (220 μm in width and 100 μm in depth, 600 μm in length on each side of hexagon) were arranged in a honeycomb pattern (HMCS) and covered with a gas permeable membrane (Pereflon® HP-045-30, t 30 μm, pore size 0.45 μm) made of porous polytetrafluoroethylene (pPTFE) obtained from Sumitomo Fine Polymer, Osaka, Japan. Sample gas was aspirated through the scrubber block at 200 mL min⁻¹ by a miniature airpump (mAP), CM-15-12 (Enomoto Micropump, Tokyo), while controlling the flow rate with a needle valve equipped with a flow meter (AFC; RK200-V-B-6H-AIR-0.5L/min, Kojima Instruments, Kyoto). The absorbing solution was pumped (100~150 μL min⁻¹) into the microchannel of the scrubber using a microring pump (mRP) (RP-Q1-N-P20A-DC3V, Aquatech, Osaka) equipped with Norprene® tubing (1.2 mm × 2.5 mm) for mobile analysis. In the case of stationary analysis, a peristaltic pump (Minipuls 3, Gilson, Middleton, WI) with 0.25 mm i.d. PVC tubing was used to pump the liquid. After passing through HMCS, the solution was passed through a reaction tube (PTFE, 0.38 mm i.d. × 65 cm) coiled around a 47-Ω porcelain enamel register powered to be 70°C. The coil was wrapped with an aluminum tape and a micro thermocouple was inserted (621-2158, RS-Components, Yokohama, Japan).

The fluorescence was monitored using a commercial fluorescence spectrophotometer (FP-2020 Plus, Jasco, Tokyo) with excitation and emission wavelengths of 410 and 510 nm, respectively, and slits of excitation and emission of 18 nm and a gain of 1000×. For mobile analysis, a miniature fluorescence detector with a UV-LED (emission maximum 405 nm, 99405, Led-On, Sagamihara, Japan) was developed. The LED was driven by a constant current of 20 mA. A glass capillary (i.d. 1.1 mm × t 0.2 mm; Chase Scientific Glass, Rockwood, TN) was used as the fluorescence cell. A 1.0 mm quartz optical fiber (MK-08, Sumitomo Electric Industries, Osaka) was inserted into the cell to introduce fluorescence to the photodiode OPT301 obtained from Texas Instruments. A color filter (SC46, Fujifilm, Tokyo) was pasted on the optical window of the photodiode to eliminate the scattering light (< 460 nm). The photodiode current was converted to voltage with a 470 MΩ resistor in a preamplifier board and the signal was further amplified 100 times in the main circuit board of the μGAS.

Sample air was introduced *via* a shortcut bypass to obtain measurement signal or a column packed with activated charcoal produced from coconut shells (Nacalai Tesque) to produce a blank signal. The measurement/blank was switched with a three-way solenoid valve (3SV) (MTB-3R-NN4 12VDC, Takasago Electric, Nagoya). The 3SV was off for 2 min for measurement signal and on for 3 min for blank signal (or 3.33 min and 6.67 min) in cyclic mode to obtain data every 5 or 10 min. The system also has a continuous mode, which provides a signal continuously. The former was advantageous to trace analysis, while the latter was advantageous to mobile monitoring.

If there was concern regarding interference from O_3, another 3SV with a wet scrubber composed of a Nafion tube (TT-110; i.d. 2.18 mm × o.d. 2.74 mm × effective length 200 mm; Perma Pure, NJ) jacketed with Teflon tubing (4 mm i.d. × 6 mm o.d.) was added (shown in a dashed line rectangle of Fig. 1b). Pure water was introduced in the gap between the Nafion and jacket tubes at a flow rate of approximately 1 mL min⁻¹. HCHO gas was removed completely using the wet scrubber, while O_3 was allowed to pass through.
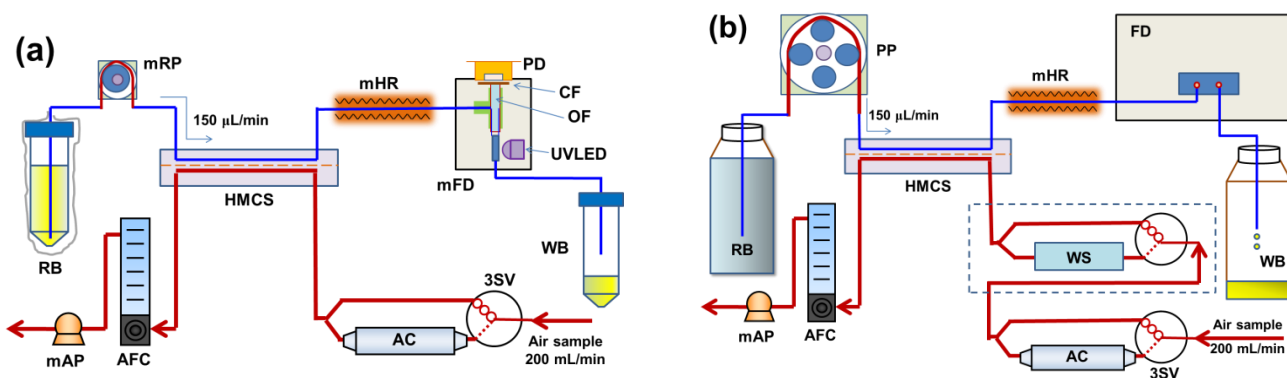
Fig. 1 Flow diagram of μGAS for mobile monitoring (a) and stationary trace measurement (b). RB: reagent bottle; mRP: microring pump; HMCS: honeycomb patterned microchannel scrubber; mHR: miniature heated reactor; mFD: miniature fluorescence detector; PD: photodiode; CF: color filter sheet; OF: optical fiber; WB: waste bottle; 3SV: three-way solenoid valve; AC: activated charcoal column; WS: wet scrubber; AFC: air flow controller; mAP: miniature airpump; PP: peristaltic pump; FD: commercial fluorescence detector; WS: wet scrubber.

Field application and validation

Mobile monitoring along a street. Mobile monitoring was performed in Kumamoto, which is a typical moderate sized city in western Japan. The entire system was placed into an aluminum box (35 cm × 29 cm × 17 cm), including the miniature airpump and a motorcycle battery. Measurements were taken in continuous mode and data were logged into the memory of the circuit board after being converted into the HCHO concentration. The ambient HCHO level was monitored by walking along a city street with the instrument. The instrument position was monitored using a global positioning system (eTrex Legend obtained from Garmin, KS) during the survey.

Forest air monitoring. HCHO in forest air was monitored in a laboratory located at Tatsuta Mountain, Kumamoto (N 32° 49', E 130° 44'), which is part of the Forestry and Forest Products Research Institute. Cars are restricted from entering the area in which the laboratory is located. Outside air was aspirated into the laboratory via a manifold and then applied to a NO_x monitor (model 42i, Nippon Thermo, Kyoto), portable GC (RGM-1, Round Science, Kyoto) and our original instrument, a single column trapping/separation–chemiluminescence detection (SCTS-CL) system for isoprene analysis.[37-39] An O_3 monitor (model 49i, Nippon Thermo) aspirated air separately because its high aspiration rate interfered with samplings of the other instruments. A PTFE filter (φ 47 mm) (PF020, Advantec, Tokyo) was placed at the inlet of the gas sampling line. The filter was covered with a polyethylene terephthalate bottle with the bottom removed to protect it from wet and dry depositions. The inlet filter and the instruments were connected with a 1/4" tube (20 m) made of PTFE–perfluoroalkoxyethylene (PFA) copolymer. The reagent solution for HCHO analysis was renewed every three days, and signals of fluorescence obtained by the commercial

Batch-wise analysis of products from PD and O_3. Products obtained by passing O_3 gas through PD solution were examined under five conditions: (a) HCHO bubbling through PD solution, (b) O_3 bubbling through PD solution, (c) O_3 bubbling through water, (d) air bubbling through PD solution, (e) air bubbling through water. In the case of test (a), 2 ppmv HCHO was passed through 10 mL of 0.03 M PD solution for 30 min.

detector were stored every second by the data logger (Midi logger GL200, Graphtec, Yokohama) together with NO_x and O_3 data.

Validation of the proposed method. Validation of the μGAS HCHO analysis was conducted during the forest air monitoring campaign. The μGAS data were compared with those collected by another method based on impinger collection followed by derivatization with o-(2,3,4,5,6-pentafluorobenzyl) hydroxylamine (PFBOA) and GC-MS analysis. Sample air was passed through an impinger containing 20 mL of water at a flow rate of 1.0 L min⁻¹ for 60 min using a mass flow controller. The impingers were arrayed and the sampling impinger was changed automatically every hour using a collection changer circuit board that was made in house. The circuit board controlled a 24 piece array composed of a three-way solenoid valve (VQ-110-6G) on two manifold blocks (VV3Q12-12) that were both from SMC, Tokyo. After collection, the absorbing solution in each impinger was transferred into a 50-mL separating funnel and 1.2 mL of 0.1% PFBOA aqueous solution was added. After 2 h of reaction in the dark, 0.32 mL of 9 M H_2SO_4, 8 g of NaCl, and 2 mL of n-hexane were added. The funnel was then shaken for 5 min, after which the samples were allowed to stand for 10 min. The aqueous phase was drained and 1 mL of the organic phase was placed in a GC vial. Next, 2 μL of the extracted sample were injected into the GC (Trace GC Ultra, Thermo, Yokohama) in splitless mode and passed through a capillary column (Inert Cap 5MS/Sil, 0.25 mm i.d. × 30 m, GL Sciences, Tokyo) with helium carrier applied at 1.0 mL min⁻¹. The column oven temperature was initially set at 50°C for 3 min, after which it was ramped up to 120°C at 15°C min⁻¹, and then to 260°C at 20°C min⁻¹, where it was held for 2.5 min. The eluted compounds were monitored using a mass analyzer (DSQ, Thermo) at m/z 181 and 195 for quantitative analysis and qualification, respectively, and the peak appeared at a retention time of ca. 7 min.

The solution was then mixed with 0.75 M acetic acid + 6 M ammonium acetate solution (AA) and Milli-Q water (1:1:1) and heated in hot water for 10 min to enable the reaction to proceed. The same procedure was performed using 65 ppmv O_3 (b) or purified air (d) instead of HCHO gas. In cases in which O_3 was used, purified air was subsequently bubbled through the solution for 10 min to remove the dissolved O_3. The products were then analyzed by HPLC-FL-ESI-MS (HPLC: Ultimate 3000, Dionex,

Sunnyvale, CA; FL: FP-2020 Plus, Jasco; ESI-MS: MSQ Plus, Thermo). The ESI conditions were as follows: probe temperature

5

Results and discussion

Reactor temperature

The effects of the reactor temperature were examined and the obtained data are shown in Fig. 2. The response intensity was small at room temperature, but increased dramatically as the reactor temperature increased from 40°C to 70°C, after which the change in intensity was small. While the peak height differed with different liquid flow rates, similar temperature effects were observed for both conditions at 100 and 150 μL min^{-1}. Above 80°C, the baseline became noisy due to bubble formation. Based on these results, 70°C was selected for further experiments. The reaction coil was effectively heated by a small resistor as described in the Experimental section and the reaction was achieved with a short reaction time (reaction coil passing time: 45 s at 100 μL min^{-1} and 30 s at 150 μL min^{-1}). The normal power consumption required to maintain the reactor temperature at 70°C at a room temperature of 25°C was only 0.37 W.

Performance of the μGAS system for measurement of HCHO

The response chart produced by the μGAS is shown in Fig. 3. HCHO gas at 0 to 20 ppbv was measured in cyclic mode, after which the test gas was passed through a bypass column and an active carbon column alternatively to obtain the signal and the baseline, respectively. The repeatability of the responses was good, and the deviations were 2.5, 1.5, 1.0, 0.78 and 0.44% for 4,

350°C, cone voltage 75V, and dwell time 0.20 s in positive mode while applying 3 kV to the needle.

8, 12, 16 and 20 ppbv HCHO, respectively. The calibration curve obtained from the data was linear and the correlation coefficient (R^2) was 0.9992. The calibration curve was linear to 100 ppbv with an R^2 of 0.9975. The delay from the change in gas concentration to the start of the signal change was 60 s, while that from the start of the signal change to attaining 90% of the final value was 50 s. The estimated limits of detection (LODs) from the results were 0.01 ppbv with the commercial fluorescence detector and 0.2 ppbv with the miniature fluorescence detector. The system was suitable to measure ppbv levels of HCHO, which are the levels found on city streets and in forest air.
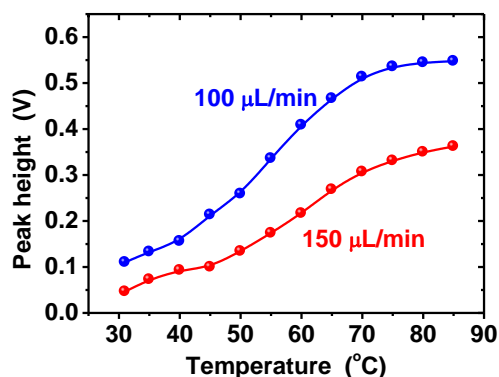

Fig. 2 Effect of reactor temperature on the response signal obtained for 20 ppbv HCHO. Note that bubbles formed above 80°C.
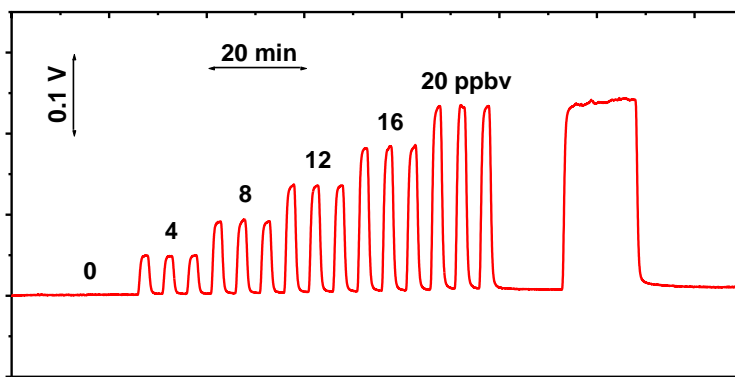

Fig. 3 Response chart obtained in the cycle mode with the commercial detector. In the test, 3SV was on for 3 min to obtain baseline and off for 2 min for response.

Mobile monitoring of atmospheric HCHO

Detailed spatial variations in atmospheric HCHO were analyzed using the μGAS. The device was light enough to walk with (5.0 kg including a 2.6-kg battery) and measurements could be made along a city street. The results of one of the measurement events (September 28, 2008) are shown in Fig. 4. During this measurement event, the operator started walking near Kumamoto Castle and walked down the castle hill to the downtown area along a castle moat. The middle of the campaign area was in the center of the city (Tori-cho), where many cars were moving

slowly or stopped at traffic signals and both sides of the road were surrounded with high buildings. After leaving the city center, the operator crossed a bridge. The HCHO levels near the castle and the bridge were obviously lower (1~5 ppbv) than those in the center, which was likely because there were fewer emission sources and wind was able to blow without interference from buildings in these areas. Conversely, high HCHO levels (maximum 32.5 ppbv) were observed in the center downtown area. Even though Kumamoto is not a large city, high HCHO levels were found in this area. The main source of HCHO was likely vehicles stopping in the street, since gases accumulated in the area surrounded by buildings. High concentrations of

pollution gases were sometimes observed in such street canyons. [40] The downtown HCHO levels were above the allowable limit (27 ppbv) determined for indoor air 8-h exposure in California. [41] Overall, the results presented here demonstrate that the HCHO level can vary dramatically in a short distance, and that the HCHO level may become high enough to be a concern to human health in downtown areas.
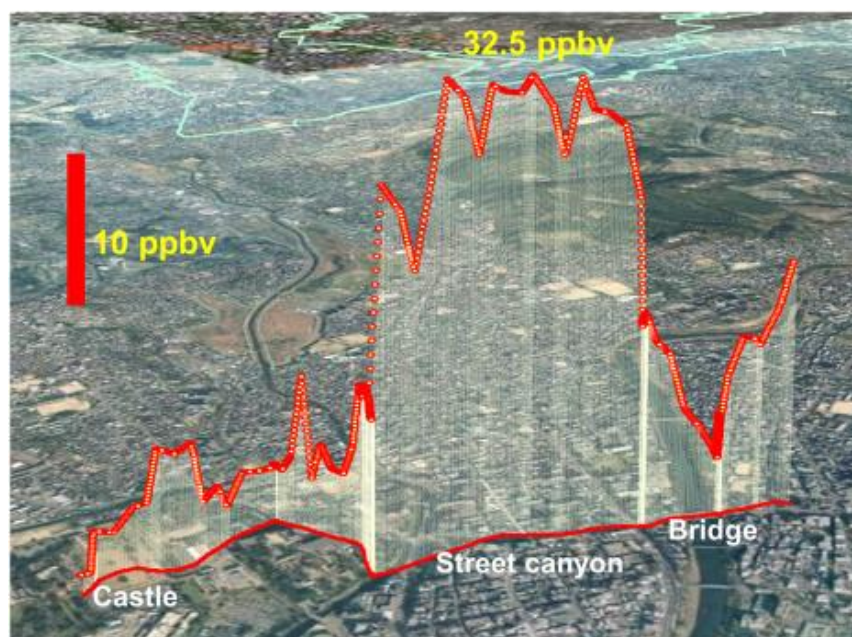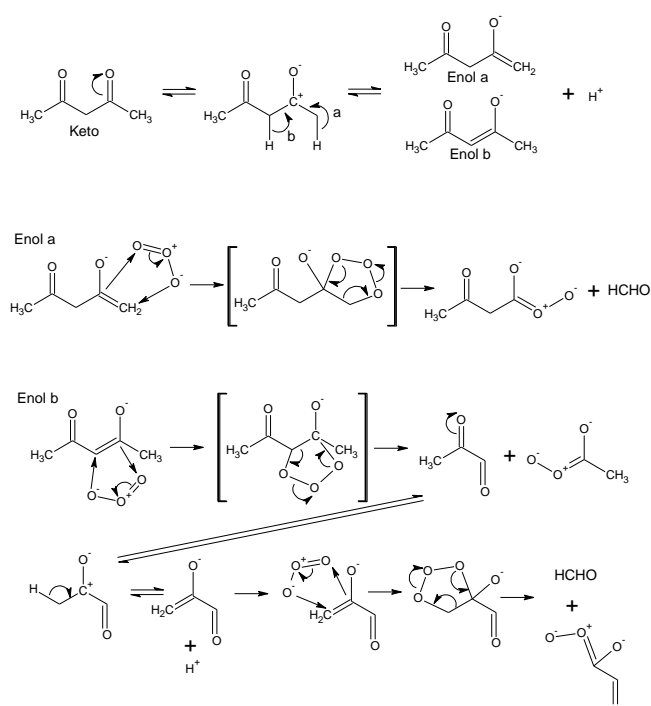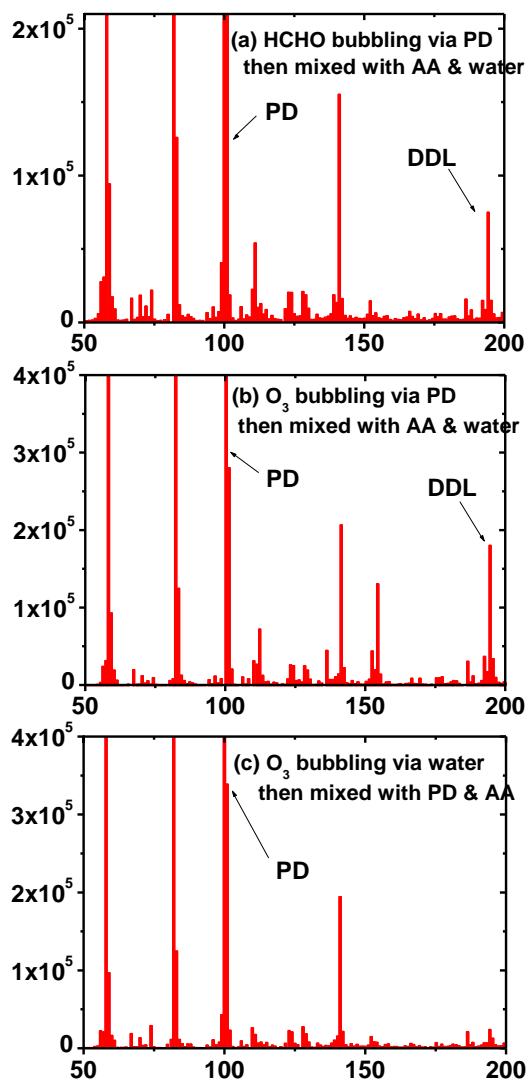

Fig. 4 Results of mobile monitoring of HCHO along a street in Kumamoto.

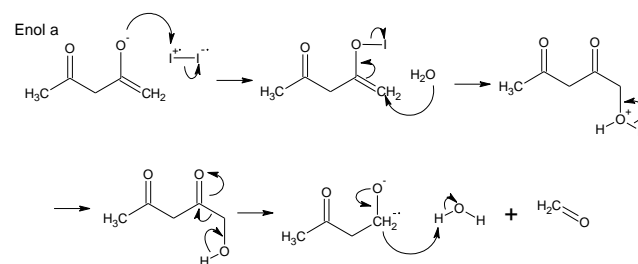### Measurement of trace HCHO under elevated O_3 conditions

Interference from O_3. While relatively high concentrations of HCHO were observed during downtown mobile monitoring, all measurements of forest air revealed only trace levels of HCHO. Specifically, the HCHO level was normally between 1 and 5 ppbv. In previous studies of trace HCHO levels, agreement between the data obtained using a coil denuder-Hantzsch reaction-HPLC and DOAS was not good, resulting in uncertainty regarding the HCHO measurements. [42,43] In the beginning of this study, the HCHO concentration was found to vary with time in a fashion similar to that of O_3. Synchronized changes of HCHO and O_3 concentrations were thought to be caused by the formation of HCHO from the reaction of hydrocarbons with O_3 and OH. The formed HCHO was one of the sources of oxidants and a reaction cycle occurred in the atmosphere between O_3 and HCHO, but O_3 was not believed to interfere with the HCHO analysis. However, subsequent testing of the μGAS in the laboratory revealed that O_3 resulted in a small and positive effect on the measured HCHO levels. This positive error was likely from a fluorescent product formed with O_3 during analysis. This is opposite to the negative error usually obtained in the conventional DNPH cartridge sampling caused by O_3. The positive O_3 interference was likely due to formation of HCHO in the absorbing solution. Kozai and Matsumoto investigated aqueous reactions of PD and O_3 and found that when 5 mM PD (250 mL) was treated with 9000 ppmv O_3 (200 mL min^{-1}), HCHO was identified as 0.27 mM, even after 5 min (the first sampling). [44] These findings indicate that HCHO was formed from aqueous PD and dissolved O_3 in a short reaction time, which was likely the same reaction that occurred in the microchannel scrubber in the present study.

The above hypothesis were confirmed by bubbling 2 ppmv HCHO, 65 ppmv O_3 and purified air separately through 20 mL of water and PD solution. After bubbling, the PD, acetic acid/ammonium acetate (AA) and water were mixed and heated in hot water for 10 min, and the compounds in the solutions were analyzed by HPLC-FL-ESI-MS. In the mass spectra, signals at m/z 100 (the base peak) and 101 were observed in all experiments, which corresponded to enol and keto forms of PD, respectively. Both HCHO and O_3 treated PD samples produced a signal at m/z 194 as in Fig. 5ab to indicate the production of 3,5-diacetyl-1,4-dihydrolutidine (DDL), while the same mass signal was not observed in the other samples as Fig. 5c (O_3 bubbled water, air bubbled PD, and air bubbled water). The mass spectrum data suggest that HCHO was produced by the reaction of PD with O_3. The HCHO production from O_3 and PD likely occurred because the scrubbing was into PD solution directly. However, the single reagent system was simple and easier to operate and obtain a stable baseline.

The di-ketone compound, PD, exists in aqueous solution as keto and enol forms as in Scheme 1. One of the enol forms is a terminal olefin (enol a), which reacts with O_3 to produce HCHO via molozonide. Ozonide may be an intermediate produced from the molozonide to generate HCHO. The other (enol b) is a major enol that also reacts with ozone to give two fragments, one of which might produce HCHO upon further reaction with O_3. These are possible mechanism to produce HCHO from PD and O_3 in our experiments and the previous work by Kozai and Matsumoto. [44]

Fig. 5 Mass spectra of HCHO and O_3 treated PD solutions. First, five sets of PD solution, AA solution and milli-Q water were prepared. HCHO, O_3 or purified air was then bubbled through the PD solution or the water. Next, the tested solution was mixed with the remaining solutions (AA and the water or the PD solution) to give a final ratio of 1:1:1. There were five combinations of gas and absorbers (a)–(e), which are described in the Experimental section. There was no obvious peak at m/z 194 in (d) and (e), which was the same as in (c).

Scheme 1 Equilibrium of PD in aqueous solution and its reaction with ozone to produce HCHO.

Scheme 2 Possible mechanism of HCHO formation from PD and I_2.

Countermeasure for O_3 interference. Although there was little interference from O_3, we decided that the interference must be removed when the O_3 level was higher than ten times the HCHO level. To accomplish this, selective removal of O_3 was examined using columns packed with solid KI. The tested columns removed O_3 quantitatively, which was confirmed by introducing 380 ppbv O_3 into the columns and using the O_3 monitor. However, the µGAS response to O_3 only decreased by 40–50%. I_2 was formed in the KI column and then likely vaporized and was then captured in the absorbing solution, where it reacted with PD. When test air was passed through a bubbler containing iodine or hypochlorous acid solution before introduction to the gas channel of the microchannel scrubber, a positive response was obtained. This result indicated that in addition to O_3, Cl_2 and I_2 reacted with PD to generate HCHO in the absorbing solution. Furthermore, loss of HCHO from the KI column was a concern during long term monitoring, and this loss might not be negligible in the case of trace HCHO measurements.

The mechanism of HCHO formation with I_2 is less certain, but can be explained as follows. Iodine acts as a Lewis acid in the aqueous phase. An electron from an enol oxygen attacks the positively charged iodine atom, resulting in connection of the atoms. The iodide then absorbs the electron to make the terminal CH_2 positive, so that the H_2O is able to bind to and remove the terminal carbon. As a result, HCHO is released from the compound (Scheme 2). Thus the KI column did not eliminate the positive O_3 interference.

Next, removal of HCHO was examined using a cylindrical wet scrubber because the KI column could not eliminate the positive errors. Henry's law constant of HCHO is 5×10^5 times higher than that of O_3 (1.1×10^{-2} M atm^{-1}). Therefore, HCHO was quantitatively removed by a short wet scrubber composed of a

Nafion tube surrounded with pure water. On the other hand, half of the O$_3$ passed through the wet scrubber. HCHO was not detected by the µGAS when the Nafion wet scrubber was placed before the microchannel scrubber. The removal efficiency of the wet scrubber was estimated to be 99% based on the spreadsheet developed by Berg et al.,[45,46] assuming that the Nafion surface acted as a perfect sink for HCHO. The low levels of HCHO and high levels of O$_3$ could be measured using PD chemistry with treatment of the air sample by two three-way solenoid valves, the active carbon column and the wet scrubber (Fig. 1b and Fig. 6). The fluorescence intensities observed when the sample gas passed through the active carbon, the wet scrubber and the bypass corresponded to the signals of the blank, O$_3$, and O$_3$ + HCHO, respectively. The concentrations of O$_3$ and HCHO were obtained from the following equations based on the data presented in Fig. 6:

$$O_3 \text{ (ppbv)} = 16.3 \text{ SIGwet (mV)} - 5.2 \qquad (2)$$

$$\begin{aligned} \text{HCHO (ppbv)} =\ & 0.0521 \text{ SIGbypass (mV)} \\ & - 0.0224 \text{ O}_3 \text{ (ppbv)} - 1.05 \end{aligned} \qquad (3)$$

SIGwet and SIGbypass were obtained when the air sample passed through the wet scrubber and bypass, respectively. The calibrations were performed immediately before each forest air monitoring event.
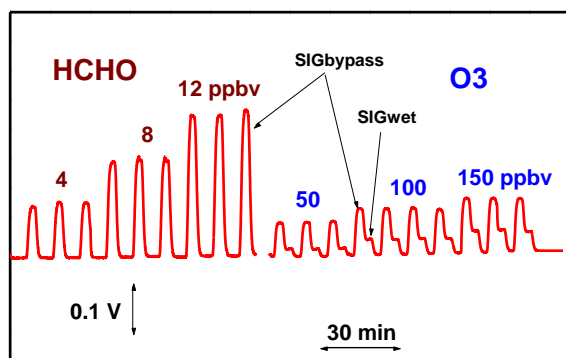

Fig. 6 Responses of the µGAS to HCHO and O$_3$.

Simultaneous measurements of HCHO and O$_3$ were previously performed by Possanizini and Palo[47] and Uchiyama et al.[48,49] using annular denuder sampling and cartridge sampling, respectively, both followed by HPLC analysis. They used well-designed chemical reactions of the two analytes. On the other hand, in this study, HCHO and O$_3$ were simultaneously analyzed in near-real time without chromatographic separations.
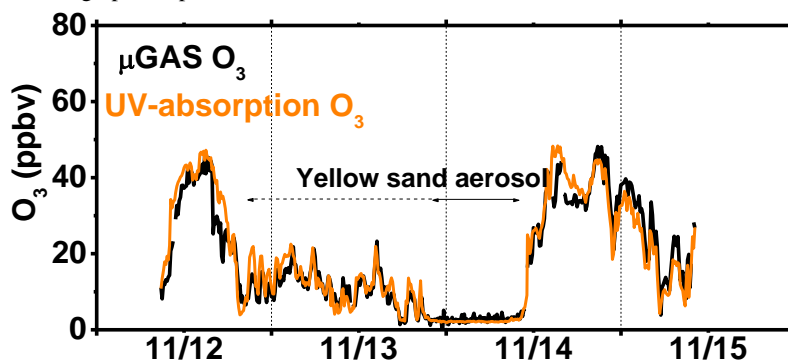
Comparison of data with those obtained with other methods. The simultaneous HCHO/O$_3$ measurement method was validated using other methods. First the O$_3$ data were compared with those obtained using a commercial O$_3$ monitor based on UV absorption (Fig. 7). Both signals matched each other well. Additionally, the results obtained using both methods clearly demonstrated that the O$_3$ levels were very low on November 14, when the yellow sand aerosols came from China. During this period, O$_3$ was likely consumed by catalytic reactions on the surface of the aerosols. Thus, the O$_3$ level varied from 2.1 to 48.3 ppbv in the 73 h period. The relationship of the O$_3$ data obtained by the two methods for every 10 min can be expressed as follows:

$$O_3 \text{ by µGAS (ppbv)} = 0.9995 \text{ O}_3 \text{ by UV (ppbv)} + 0.7975$$
$$R^2 = 0.8048 \qquad (4)$$

Although there were deviations, there was a good relationship between the data obtained using the two methods. As a result, PD chemistry followed by fluorescence detection can be used for O$_3$ monitoring as well.

HCHO was also measured by derivatization with PFBOA followed by GC-MS analysis as described in the Experimental section. Salthammer and Mentese showed good agreement of data obtained using the PD chemistry and by the DNPH method.[50] In our experiments, sensitivity of the DNPH method was not sufficient for forest HCHO monitoring so that the PFBOA method was used. The results are compared in Fig. 8. The HCHO levels measured using the modified µGAS agreed well with those measured using PFBOA-GC-MS, but the µGAS had a better time resolution. Specifically, the time resolution of the µGAS was 10 min during the forest monitoring, while PFBOA-GC-MS required 1 h to obtain the same sensitivity. The data were obtained from measurements taken in the forest and an experiment in our laboratory in which outside air was continuously introduced through a window. The relationship between the data obtained using the µGAS and PFBOA-GC-MS systems for the forest and laboratory experiments is shown in panel b. The following equation described the relationship between these datasets:

$$\text{HCHO by µGAS (ppbv)} = 1.033 \text{ HCHO by GC (ppbv)} - 0.0886$$
$$n = 36, R^2 = 0.9195 \qquad (5)$$

Although the principles involved in these methods differed, the results obtained using them agreed well. The measurement in which the µGAS was used with O$_3$ compensation was simple and provided data in near real time, while the HCHO data at trace levels agreed with those obtained by PFBOA-GC-MS.
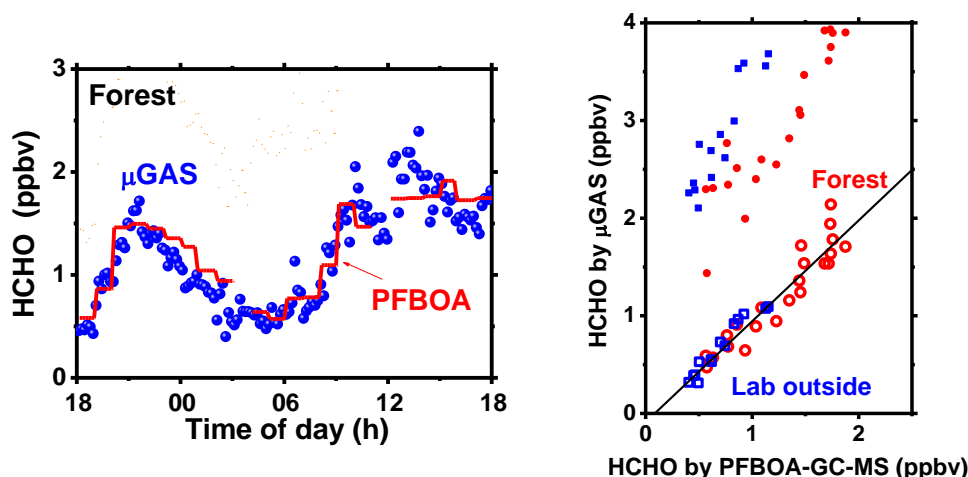

Fig. 7 Comparison of O$_3$ data obtained using the modified-µGAS system and commercial O$_3$ monitoring based on UV-absorption.

Fig. 8 Validation of the HCHO data using the PFBOA-GC-MS method; changes in HCHO level with time obtained in the forest by the μGAS (●) and PFBOA-GC-MS (—) in panel (a) and relationship of the data obtained using the two methods to analyse air sampled from outside the laboratory (□) and the forest (○)(b); values on the y-axis in (b) are averages of six data points obtained using the μGAS during 1-h of PFBOA sampling. Solid symbols in (b) indicate data obtained without wet scrubber compensation.

Production and loss of formaldehyde in forest air

Air monitoring was performed in the forest. Daily and seasonal variations of isoprene were shown in a previous study[34] in which HCHO data were presented as one of the related compounds. Typical time variations in HCHO are shown in Fig. 9 together with biogenic volatile organic compounds (BVOCs) and O₃ obtained August 25–27, 2009. The time variation of emission and loss of isoprene in the same day were discussed in a previous paper. In the present study, the production and loss of HCHO in the forests is discussed based on data obtained in the same campaign.

HCHO is formed by oxidation of volatile organic compounds. Therefore, the HCHO production rate, P_{HCHO}, can be expressed by eq. 6, which includes the VOC concentrations $[BVOC]_j$, oxidant concentrations $[Oxidant]_i$, reaction rate constants k_{ij} and yields of HCHO in the reactions γ_{ij}.[51,52]

$$P_{HCHO} = \sum_i \sum_j \left(\gamma_{ij} k_{ij} [BVOC]_j [Oxidant]_i \right) \quad (6)$$

For estimation of the HCHO production rate, isoprene, α-pinene, and β–pinene were considered as the BVOCs that were primarily observed in the campaigns, and OH and O₃ were the oxidants. The OH concentration was estimated from a graph for summer OH in the literature[53] as the manner of the previous work,[54] and the other concentrations, ambient temperature and solar irradiation were measured simultaneously. The parameters, k_{ij} and γ_{ij}, used are shown in Table 1. Variations in HCHO production were estimated from these field results and detailed variations of the production via reaction of isoprene with OH radical are given in Fig. 10. The maximum production occurred around 2 pm every day because both of these compounds are formed with sunlight. HCHO was primarily produced in the daytime. The daily production rate was obtained by integration of the variation curve. The daily production rates via the other reactions were estimated in the same way and summarized in Table 1. The total HCHO production was 11.0 ± 1.0 ppbv d⁻¹. The major production process was isoprene/OH, which accounted for 70.4% of the total production. The HCHO yield of the isoprene/O₃ reaction was high (0.90) and the O₃ concentration also affected the HCHO

production. The HCHO production from α-pinene with OH and O₃ was comparable, being 0.89 ± 0.09 and 1.00 ± 0.24 ppbv d⁻¹, respectively. The production from β–pinene/O₃ was negligible.
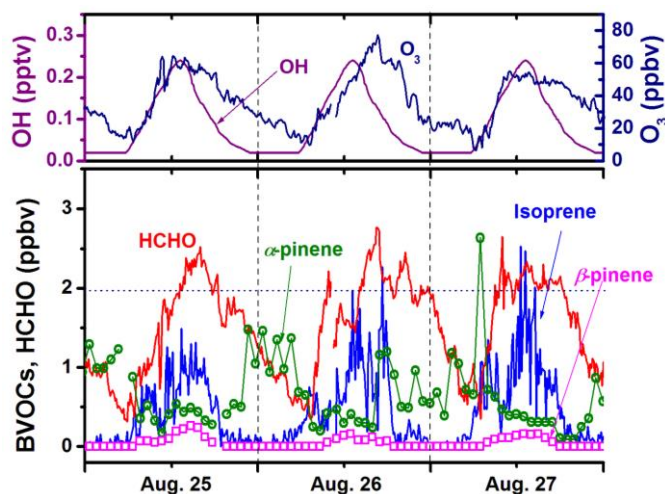

Fig. 9. Diurnal variations in HCHO and the related compounds. The OH concentrations were from ref. 54.
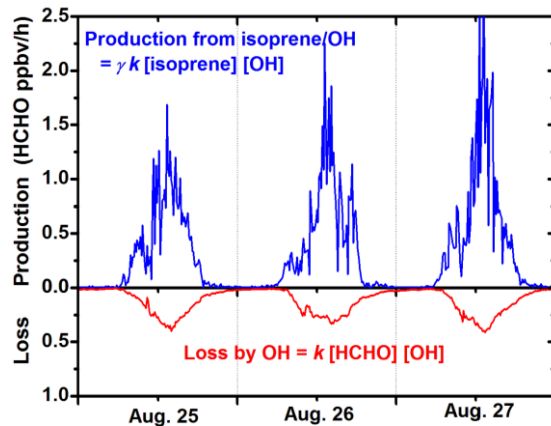

Fig. 10. Diurnal variations in the HCHO production via isoprene/OH reaction and the HCHO loss by OH.

Table 1 Production and loss of HCHO by BVOC/oxidant reactions.

| Reaction | Rate constant, k (cm^3 molecule^{-1} s^{-1}) | | Yield* | HCHO production, P_{HCHO} | | |
		at 298K	γ	Max ppbv h^{-1}	Daily ppbv d^{-1}	%
Isoprene + OH	2.7×10^{-11}exp(390/T)	1.0×10^{-10}	0.55	2.80	7.74 ± 1.26	70.4
Isoprene + O$_3$	1.03×10^{-14}exp(-1995/T)	1.3×10^{-17}	0.90	0.15	0.53 ± 0.05	4.9
α-pinene + OH	1.2×10^{-11}exp(440/T)	5.3×10^{-11}	0.19	0.14	0.89 ± 0.09	8.2
α-pinene + O$_3$	6.3×10^{-16}exp(-580/T)	9.0×10^{-17}	0.25	0.18	1.00 ± 0.24	9.3
β–pinene + OH	–	7.8×10^{-11}	0.51	0.21	0.73 ± 0.18	6.8
β–pinene + O$_3$	–	1.5×10^{-17}	0.65	0.01	0.05 ± 0.02	0.5
Total				3.17	11.0 ± 1.0	100
Loss						
HCHO + OH	5.4×10^{-12}exp(135/T)	8.5×10^{-12}	–	0.41	−2.86 ± 0.15	

* Yield is the mol ratio of produced HCHO to source compound BVOC.

The HCHO produced in the forest air decomposed via many pathways, including photolysis, chemical reactions and dry deposition.[3] In the chemical reactions, HCHO reacts with OH (k 8.5×10^{-12} cm^3 molecules^{-1} s^{-1}),[55] O$_3$ (2.1×10^{-24}),[56] NO$_3$ (5.8×10^{-16}),[55] and HO$_2$ (5.0×10^{-14}).[55] The chemical decomposition rates estimated for typical oxidant concentrations (OH 0.2 pptv, O$_3$ 60 ppbv, NO$_3$ 3 pptv, HO$_2$ 4 pptv) had the following ratio: OH 1.3×10^7: O$_3$ 1.0: NO$_3$ 1.4×10^5: HO$_2$ 1.5×10^6. Thus, decomposition with OH was dominant in the chemical reactions as Sumner et al.[3] stated. Additionally, photolysis and dry deposition were the major fate of atmospheric HCHO during daytime and nighttime, respectively, and the loss of HCHO (L_{HCHO}) could be expressed by the photolysis rate constant J, the second order rate constant k, the dry deposition rate V_d (m s^{-1}) and the height of the boundary layer H as follows:

$$L_{HCHO} = J\,[\text{HCHO}] + k\,[\text{OH}][\text{HCHO}] + V_d\,[\text{HCHO}]\,H^{-1} \qquad (7)$$

There are two photolysis processes that produce (H· and HCO·) and (H$_2$ and CO) (in both $\lambda < 330$ nm),[52] and the respective rate constants, J_{la} and J_{lb}, are expressed with photosynthetically active radiation (PAR, μmol m^{-2} s^{-1}) as follows (PAR can be driven by multiplying 4.57 to solar insolation (W m^{-2})):[57]

$$J_{la}(\text{s}^{-1}) = -2.67\times10^{-15}(\text{PAR})^3 + 9.65\times10^{-12}(\text{PAR})^2 + 6.47\times10^{-8}(\text{PAR}) - 1.25\times10^{-8} \qquad (8)$$

$$J_{lb}(\text{s}^{-1}) = -3.25\times10^{-15}(\text{PAR})^3 + 8.12\times10^{-12}(\text{PAR})^2 + 1.90\times10^{-8}(\text{PAR}) - 1.37\times10^{-8} \qquad (9)$$

We attempted to determine the daily variations in the HCHO loss. However, many assumptions regarding the parameters for calculation of L_{HCHO} were required and reasonable estimation was difficult. Nevertheless, it can be said that the first and second terms in eq. 7 occur during daytime and are generally proportional to the sunlight intensity. The last term, dry deposition, was dominant during nighttime.

As mentioned above, the main chemical production and loss of HCHO were a result of reaction of isoprene with OH and chemical decomposition by OH, respectively, which are both proportional to the OH concentration. Although the OH level was estimated from the literature, the ratio of production/loss by OH is not related to the OH concentration. Detailed data describing isoprene and HCHO are presented in this study and time variations with a good resolution were obtained as in Fig. 10. During monitoring of the forest site, isoprene was the dominant BVOC. While both the rates of production from isoprene/OH and loss by OH increased as the OH level increased, the production rate was higher than the loss rate. The three day data indicated

that the daily production and loss by OH were 7.74 ± 1.26 and 2.86 ± 0.15 ppbv d^{-1}, respectively. While the OH radical contributed to both the production and loss, the contribution to the HCHO production was three times greater than the HCHO loss. Isoprene is a reactive compound that contributes more to the production of HCHO than other BVOCs. These suggest that HCHO production may be greater in broad-leaved tree forests than conifer forests.

Conclusions

A portable and highly sensitive device for atmospheric HCHO analysis was developed. The information obtained is itemized below.

- The developed μGAS was suitable for mobile analysis of HCHO along a street in an urban area. The local HCHO levels in the downtown area varied dramatically in a short distance, and relatively high concentrations of HCHO were observed in the street canyon, which may affect human health.
- The results revealed that PD chemistry for HCHO detection at trace levels was subject to interference from high concentrations of O$_3$. This was likely due to production of HCHO by the reaction of PD with O$_3$ in the absorbing solution. Although a KI cartridge removed the O$_3$, the positive interference could not be removed by the cartridge owing to the formation of I$_2$ that vaporized and moved into the absorbing solution to produce HCHO via its reaction with PD. This interference was addressed by incorporation of a wet denuder for selective HCHO removal.
- The developed μGAS could be used to monitor trace levels of atmospheric HCHO in the forest every 10 min, and the data generated by the μGAS agreed with those obtained by the PFBOA derivatization-GC-MS conducted at 30 min intervals and the offsite laboratory analysis.
- Analysis of the data obtained in the forest revealed that the HCHO production by the isoprene/OH reaction and the HCHO loss by reaction with the OH radical increased during daytime. The production was about three times higher than the chemical loss during the summer measurement period.

The analytical device developed in this study is expected to be useful for monitoring of atmospheric and indoor HCHO.

References

1   T. Salthammer, S. Mentese, R. Marutzky, *Chem. Rev.*, 2010, **110**, 2536–2572.
2   H. Zhao, Y. Ge, C. Hao, X. Han, M. Fu, L. Yu, A.N. Shah, *Sci. Total Environ.*, 2010, **408**, 3607–3613.
3   A.L. Sumner, P.B. Shepson, T.L. Couch, T. Thornberry, M.A. Carroll, S. Sillman, M. Pippin, S. Bertman, D. Tan, I. Faloona, W. Brune, V. Young, O. Cooper, J. Moody, W. Stockwell, *J. Geophys. Res.*, 2001, **106**, D20, 24387–24405.
4   M. Possanzini, V. Di Palo, A. Cecinato, *Atmos. Environ.*, 2002, **36**, 3195–3201.
5   A.M. Macdonald, P.A. Maker, K.G. Anlauf, K.L. Hayden, J.W. Bottenheim. D. Wang, T. Dann, *J. Geophys. Res.*, 2001, **106**, D23, 32361–32374.
6   R.B. Chatfield, X. Ren, W. Brune, J. Schwab, *Atmos. Environ.*, 2010, **44**, 5395–5406.
7   W.L. Chameides and D.D. Davis, *Nature*, 1983, **304**, 427–429.
8   D.J. Jacob, *J. Geophys. Res.*, 1986, **91**, D9, 9807–9826.
9   P. Khare, G.S. Satsangi, N. Kumar, K.M. Kumari, S.S. Srivastava, *Atmos. Environ.*, 1997, **23**, 3867–3875.
10 M. Possanzini, V. Di Palo, M. Petricca, R. Fratarcangeli, D. Brocco, *Atmos. Environ.*, 1996, **30**, 3757–3764.
11 S.M. Corrêa, E.M. Martins, G. Arbilla, *Atmos. Environ.*, 2003, **37**, 23–29.
12 Z.-Y Gu, G. Wang, X.-P. Yan, *Anal. Chem.*, 2010, **82**, 1365–1370.
13 A.L. Lazrus, K.L. Fong, J.A. Lind, *Anal. Chem.*, 1988, **60**, 1074–1080.
14 H.-W. Jacobi, M.M. Frey, M.A. Hutterli, R.C. Bacles, O. Schrems, N.J. Cullen, K. Steffen, C. Koehler, *Atmos. Environ.*, 2002, **36**, 2619–2628.
15 K. Riedel, R. Weller, O. Schrems, *Phys. Chem. Chem. Phys.*, 1999, **1**, 5523–5527.
16 F. Vianello, R. Boscolo-Chio, S. Signorini, A. Rigo, *Biosens. Bioelectron.*, 2007, **22**, 920–925.
17 J. Li, P.K. Dasgupta, Z. Genfa, M.A. Hutterli, *Field Anal. Chem. Technol.*, 2001, **5**, 2–12.
18 P.K. Dasgupta, S. Dong, H. Hwang, H.-C. Yang, Z. Genfa, *Atmos. Environ.*, 1988, **22**, 949 – 963.
19 Y. Komazaki, Y. Narita, S. Tanaka, *Analyst*, 1998, **123**, 2343–2349.
20 L. Allou, L.El Maimouni, S.Le Calvé, *Atmos. Environ.*, 2011, **45**, 2991–2998.
21 K. Toda, K. Yoshioka, K. Mori, S. Hirata, *Anal. Chim. Acta*, 2005, **531**, 41–49.
22 J. Li, P. K. Dasgupta, W. Luke, *Anal. Chim. Acta*, 2005, **531**, 51–68.
23 K. Motyka, P. Mikuška, *Anal. Chim. Acta*, 2004, **518**, 51–57.
24 J. Li, P.K. Dasgupta, Z. Genfa, M.A. Hutterli, *Field Anal. Chem. Technol.*, 2001, **5**, 2–12.
25 T. Sakai, S. Tanaka, N. Teshima, S. Yasuda, N. Ura, *Talanta*, 2002, **58**, 1271–1278.
26 P.K. Dasgupta, J. Li, G. Zhang, W.T. Luke, W.A. Mcclenny, J. Stutz, A. Fried, *Environ. Sci. Technol.*, 2005, **39**, 4767–4783.
27 S. Ohira, K. Toda, *Lab Chip*, 2005, **5**, 1374–1739.
28 K. Toda, T. Koga, J. Kosuge, M. Kashiwagi, H. Oguchi, T. Arimoto, *Anal. Chem.*, 2009, **81**, 7031–7037.
29 K. Toda, Y. Hato, S. Ohira, T. Namihira, *Anal. Chim. Acta*, 2007, **603**, 60–66.
30 S. Ohira, K. Toda, *Anal. Sci.*, 2006, **22**, 61–65.
31 S. Ohira, K. Someya, K. Toda, *Anal. Chim. Acta*, 2007, **588**, 147–152.
32 S. Ohira, K. Toda, *Anal. Chim. Acta*, 2008, **619**, 143–156.
33 K. Toda, P.K. Dasgupta, in *Comprehensive Analytical Chemistry*, ed. S.D. Kolev, I.D. Mckelvie, Elsevier, Amsterdam, 2008, vol. 54, ch. 22, pp.639–683.
34 K. Toda, K. Hirota, W. Tokunaga, D. Suda, Y. Gushiken, S. Ohira, *Bunseki Kagaku*, 2011, **60**, 489–498.
35 S. Dong, P.K. Dasgupta, *Environ. Sci. Technol.*, 1986, **20**, 637–640.
36 L.C. Short, T. Benter, *J. Chem. Educ.*, 2006, **83**, 1233–1236.
37 M.A.K. Azad, S. Ohira, K. Toda, *Anal. Chem.*, 2006, **78**, 6252–5259.
38 S. Ohira, J. Li, W.A. Lonneman, P.K. Dasgupta, K. Toda, *Anal. Chem.*, 2007, **79**, 2641–1649.
39 K. Toda, K. Hirota, W. Tokunaga, D. Suda, Y. Gushiken, S. Ohira, *Bunseki Kagaku*, 2011, **60**, 489–498.
40 X. Pang, X. Lee, *Atmos. Environ.*, 2010, **44**, 2098–2106.
41 California Air Resources Board, Formaldehyde in the home, in *Indoor air quality guideline No.1*, CARB, 2004, pp.1–16 (http://www.arb.ca.gov/research/indoor/formaldGL08-04.pdf).
42 A.J. Weinheimer, Chemical methods: chemiluminescence, chemical amplification, electrochemistry, and derivatization, in *Analytical Techniques for Atmospheric Measurement*, ed. D.E. Heard, Blackwell Publishing, 2006, pp.311–360.
43 L.M. Cárdenas, D.J. Brassington, B.J. Allan, H. Coe, B. Alicke, U. Platt, K.M. Wilson, J.M.C Plane, S.A. Penkett, *J. Atmos. Chem.*, 2000, **37**, 53–80.
44 S. Kozai, H. Matsumoto, *Mizukankyo Gakkaishi*, 1997, **20**, 539–547.
45 J.M. Berg, D.L. James, C.F. Berg, K. Toda, P.K. Dasgupta, *Anal. Chim. Acta*, 2010, **664**, 56–61.
46 K. Toda, T. Koga, T. Tanaka, S. Ohira, J.M. Berg, P.K. Dasgupta, *Talanta*, 2010, **82**, 1870–1875.
47 M. Possanzini, V.D. Palo, *Chromatographia*, 1988, **25**, 895–898.
48 S. Uchiyama, Y. Otsubo, *Anal. Chem.*, 2008, **80**, 3285–3290.
49 S. Uchiyama, S. Naito, M. Matsumoto, Y. Inaba, N. Kunugita, *Anal. Chem.*, 2009, **81**, 6552–6557.
50 T. Salthammer, T. Mentese, *Chemosphere*, 2008, **73**, 1351–1356.
51 W. Choi, I. C. Faloona, N. C. Bouvier-Brown, M. McKay, A. H. Goldstein, J. Mao, W. H. Brune, B.W. LaFranchi, R. C. Cohen, G. M. Wolfe, J. A. Thornton, D. M. Sonnenfroh, D. B. Millet, *Atmos. Chem. Phys.*, 2010, **10**, 8761–8781.
52 A. L. Sumner, P. B. Shepson, T. L. Couch, T. Thornberry, M. A. Caroll, S. Sillman, M.Pippin, S. Bertman, D. Tan, I. Faloona, W. Brune, V. Young, O. Cooper, J. Moody, W. Stockwell, *J. Geophys. Res.*, 2001, **106**, 24387–24405.
53 X. Rena, W.H. Brunea, J. Maoa, M.J. Mitchella, R.L. Leshera, J.B. Simpasa, A.R. Metcalfa, J.J. Schwabb, C. Caib, Y. Lib, K.L. Demerjianb, H.D. Feltonc, G. Boyntonc, A. Adamsc, J. Perryc, Y. Hed, X. Zhoud, J. Hou, *Atmos. Environ.*, 2006, **40**, S252–S263.
54 Y.C. Lin, Y.Y. Lan, B.-J. Tsuang, G. Engling, *Atmos. Environ.*, 2008, **42**, 4320–4331.
55 S.P. Sander, D.M. Golden, M.J. Kurylo, G.K. Moortgat, P.H. Wine, A.R. Ravishankara, C.E. Kolb, M.J. Molina, B.J. Finlayson-Pitts, R.E. Huie, Chemicalkinetics and photochemical data for use in atmospheric studies evaluation No.15. NASA Jet Propulsion Laboratory Publication 06-2, 2006.
56 J. Zhang, W.E. Wilson, P.J. Lloy, *Environ. Sci. Technol.*, 1994, **28**, 1975–1982.
57 C.P. Jacovides, F.S. Tymvios, D.N. Asimakopoulos, K.M. Theofilou, S. Pashiardes, *Theor. Appl. Climatol.*, 2003, **74**, 227–233.